# Improved Daytime Column-Integrated Precipitable Water Vapor from Vaisala Radiosonde Humidity Sensors

K. E. CADY-PEREIRA AND M. W. SHEPHARD

*Atmospheric and Environmental Research, Inc., Lexington, Massachusetts*

D. D. TURNER

*SSEC, University of Wisconsin—Madison, Madison, Wisconsin*

E. J. MLAWER AND S A. CLOUGH

*Atmospheric and Environmental Research, Inc., Lexington, Massachusetts*

T. J. WAGNER

*SSEC, University of Wisconsin—Madison, Madison, Wisconsin*

(Manuscript received 14 May 2007, in final form 30 October 2007)

ABSTRACT

Accurate water vapor profiles from radiosondes are essential for long-term climate prediction, weather prediction, validation of remote sensing retrievals, and other applications. The Vaisala RS80, RS90, and RS92 radiosondes are among the more commonly deployed radiosondes in the world. However, numerous investigators have shown that the daytime water vapor profiles measured by these instruments present a significant dry bias due to the solar heating of the humidity sensor. This bias in the column-integrated precipitable water vapor (PWV), along with variability due to calibration, can be removed by scaling the humidity profile to agree with the PWV retrieved from a microwave radiometer (MWR), as has been demonstrated by several previous studies. Infrared radiative closure analyses have shown that the MWR PWV does not present daytime versus nighttime differences; thus, scaling by the MWR is a possible approach for removing the daytime dry bias. However, MWR measurements are not routinely available at all radiosonde launch sites. Starting from a long-term series of sonde and MWR PWV measurements from the Atmospheric Radiation Measurement (ARM) Southern Great Plains (SGP) site, the authors have developed a simple correction to the column-integrated sonde PWV, derived from an analysis of the ratio of the MWR and sonde measurements; this correction is a function of the atmospheric transmittance as determined by the solar zenith angle, and it effectively removes the daytime dry bias at all solar zenith angles. The correction was validated by successfully applying it to an independent dataset from the ARM tropical western Pacific (TWP) site.

## 1. Introduction

Water vapor is the most abundant and the most highly variable greenhouse gas in the atmosphere. This temporal and spatial variability greatly affects the radiative fluxes at the surface and at the top of the atmosphere (TOA) and on the radiative heating rates at all layers of the atmosphere. In addition, the distribution of water vapor is a fundamental driving force behind the formation of clouds and precipitation. The pivotal importance of water vapor to these atmospheric processes demands that numerical weather prediction and climate models use accurate water vapor profiles as part of their data assimilation process. The validation of retrieved water vapor from remote sensing instruments also requires accurate ground truth. Traditionally, the profiles required for these tasks have been obtained

*Corresponding author address:* Karen Cady-Pereira, Atmospheric and Environmental Research, Inc., 131 Hartwell Ave., Lexington, MA 02421.
E-mail: cadyp@aer.com

DOI: 10.1175/2007JTECHA1027.1

from water vapor radiosondes launched from the global network of weather stations, among them the Vaisala RS80 and more recently RS90 and RS92.

Radiosonde water vapor profiles are often considered "truth," but inconsistencies between radiosondes and other instruments, between different types of radiosondes, or even between radiosonde profiles recorded by the same type of instrument have been repeatedly noted (Turner et al. 2003, and references therein). These differences in the radiosonde water vapor profiles have a significant impact. For example, Zipser and Johnson (1998) noted serious, site-specific biases in humidity profiles during the Tropical Ocean Global Atmosphere Coupled Ocean–Atmosphere Response Experiment (TOGA COARE) observations. The magnitude of the biases required that the TOGA COARE team develop correction algorithms, which used an independent surface humidity measurement (Wang et al. 2002). Starting from TOGA COARE measurements, Guichard et al. (2000) showed that the dry bias in the sonde profiles led to severe underestimation of convective available potential energy (CAPE) and overestimation of convective inhibition (CIN), which in turn led to a prediction of an unphysical and not observed stabilization of the tropical atmosphere. Correcting the measured humidity profiles yielded much more accurate values of CAPE and CIN and more realistic convective prediction. The impact of biases in the humidity profiles extends far beyond local convective behavior. While the global anthropogenic radiative forcing is estimated to be 1.6 W $m^{-2}$ (Solomon et al. 2007), the actual effect may be greater because of a strong water vapor positive feedback (Raval and Ramanathan 1989). Guichard et al. (2000), again using the TOGA COARE soundings, showed that uncorrected sonde profiles underestimated the surface downward longwave flux by 2.0 W $m^{-2}$ and overestimated the TOA upward longwave flux by 1.0 W $m^{-2}$ under cloudy conditions, and by twice as much under clear conditions; these results highlight the importance of accurate humidity profiles for long-term climate modeling. Thus, determining the source of these biases in the sonde humidity profiles and developing methods to remove them has been the focus of much research in the last 15 yr.

The objective of this study is to examine techniques for improving the daytime column-integrated precipitable water vapor (PWV) obtained from the Vaisala RS80-H and RS90/92 sondes. The long-term day–night accuracy of PWV from the radiosondes is analyzed relative to accurate coincident PWV measurements retrieved from a microwave radiometer (MWR). As we discuss in section 2, the MWR PWV has been validated previously through radiative closure studies and thus provides a measurement of PWV that is independent of sonde measurements. We focus mainly on the Vaisala RS90 and RS92 radiosondes launched from the Atmospheric Radiation Measurement (ARM) program's Southern Great Plains (SGP) site over the 2001–05 period, but also include results from a smaller dataset collected in the tropical western Pacific (TWP). In addition, the results from the older RS80-H radiosondes will be discussed briefly. We first review the technique of adjusting PWV obtained from the sonde profiles by scaling by the PWV retrieved from the microwave radiometer, then compare the forward calculations of a radiative transfer model driven by these adjusted profiles with spectral measurements from an infrared interferometer. This analysis suggests that the radiosonde humidity sensor has a strong diurnal bias, with the daytime data having a substantial dry bias relative to nighttime data. We next look closely at the daytime dry bias, described by Miloshevich et al. (2006) during AIRS Water Vapor Experiment—Ground (AWEX-G) and, more recently, by Vömel et al. (2007) during the Ticosonde campaign in Alajuela, Costa Rica, in July 2005, and the Water Vapor Validation Experiments (WAVES) campaign, and derive a simple correction factor calculated from the solar zenith angle. No attempt was made to find a height-dependent correction factor for this daytime dry bias.

## 2. Using the MWR to improve radiosonde humidity profiles

The Department of Energy ARM program maintains facilities at several locations around the world that have the principle objective of providing an extensive suite of atmospheric and radiative measurements for use in improving radiative transfer calculations (Ackerman and Stokes 2003). At the ARM SGP site in Oklahoma, (36.606°N, −97.485°E), radiosondes are regularly launched 4 times a day, and more frequently during intensive observation periods (IOPs). At the same location, there is a radiometrics microwave radiometer that continuously (every 20 s) measures the sky downwelling brightness temperature at 23.8 and 31.4 GHz. Water vapor absorption and emission dominate the signal in the 23.8-GHz channel, which is on the wing of the 22.2-GHz water vapor line, while the 31.4-GHz channel is mainly sensitive to liquid water emission. From these two measurements, accurate PWV and cloud liquid water (CLW) values can be obtained from a physical retrieval approach (Turner et al. 2007) that utilizes the validated microwave radiative transfer model MonoRTM (Clough et al. 2005). Years of experience

with the MWR at ARM have shown that the MWR PWV is accurate and stable (Liljegren 2000), and it can thus be used to evaluate the PWV from the sonde.

The dry bias in the water vapor profiles from the Vaisala RS80 radiosondes observed during TOGA COARE was also noted at the ARM SGP site when comparisons of thousands of sonde PWV measurements were made with corresponding values retrieved from the MWR (Turner et al. 2003). These comparisons yielded an average 5% dry bias. Eventually, this dry bias was traced to contamination from the Styrofoam packaging of the sensor (Wang et al. 2002); after June 2000, Vaisala RS80 sondes were shipped with a sealed sensor cap and the contamination problem was mostly solved. However, the change in packaging neither eliminated the large sonde-to-sonde variability (peak-to-peak differences greater than 25%) in the MWR/sonde ratio (Turner et al. 2003) nor the daytime-only bias, which will be discussed in detail below. This experience led ARM to create a scaled sonde profile product, whereby the sonde volume mixing ratio at every level is scaled by the ratio between the MWR PWV and the sonde PWV (the MWR scale factor), and then converted to RH using the sonde temperature and pressure values. This approach assumes that error in humidity is independent of height, which is supported by dual sonde observations during special water vapor IOPs at ARM in 1996 and 1997 (Turner et al. 2003; Revercomb et al. 2003).

This MWR-scaling approach was validated using a radiative transfer closure experiment in the infrared (Turner et al. 2003, 2004). This closure experiment used the unscaled and MWR-scaled RS80-H radiosondes to drive the line-by-line radiative transfer model (LBLRTM; Clough et al. 2005); these calculations were then compared against the high-spectral-resolution observations from the Atmospheric Emitted Radiance Interferometer (AERI; Knuteson et al. 2004a,b) from 550 to 3000 $cm^{-1}$. In this experiment, a population of 230 clear sky cases from the October 1998 to September 2001 period was analyzed. The residuals between the AERI measurements and LBLRTM calculations were much lower for the scaled sonde profiles, and the standard deviation of the residuals was a factor of 2 smaller, indicating the value of the MWR-scaling technique in reducing the variability in radiosonde moisture profiles.

The scaling of radiosonde profiles by the MWR over a longer infrared radiative closure dataset (2000–04), during which the sondes deployed were RS90s, seemingly provides mixed results (Fig. 1). The mean residuals are small, but the infrared spectral residuals, which use the MWR-scaled radiosonde results as input into the LBLRTM, show greater biases than the nominal radiosonde results. The mean residuals from the unscaled radiosonde profiles are very close to zero for all three PWV ranges, while the residuals from the MWR-scaled profiles become increasingly more negative in the atmospheric window region as the PWV increases. The negative residuals at larger PWV amounts suggest either that the PWV amount retrieved from the MWR is too large (by approximately 2%), resulting in too much water vapor being used in the LBLRTM calculation, or that the water vapor continuum absorption is too large (by approximately 4%). The source of the discrepancy is still under active investigation; however, work currently in progress suggests that the larger residuals at high water vapor value for the scaled sondes are due to errors in the water vapor infrared spectroscopic parameters used by LBLRTM.

The mean spectral residuals for the nominal sondes in Fig. 1 disguise the true nature of the data: the standard deviation results indicate significant variability in the sonde profile measurements, a variability that is reduced via scaling by the MWR PWV. Further insight is provided in Fig. 2, where the residuals in a single microwindow channel at 845 $cm^{-1}$ are plotted as a function of PWV and separated into nighttime (0000–1200 UTC) and daytime (1200–2400 UTC) sets. These results demonstrate that the nominal radiosonde water vapor observations have a significant diurnal character, with the daytime results having positive residuals (implying too little water vapor in the profiles provided by the radiosondes); on the other hand, the scaled radiosonde profiles do not present a diurnal character; furthermore, the nominal nighttime residuals are very similar to the scaled residuals, indicating that the trend of water vapor in the nominal nighttime and daytime and nighttime-scaled residuals arises from an error in the forward model (LBLRTM). These observations confirm that the daytime dry bias observed in the sonde humidity profiles is due to a problem with the sonde measurement; scaling by the MWR not only reduces the scatter in the AERI–LBLRTM residuals but also eliminates the daytime dry bias. This result, shown here for the Vaisala RS90 radiosonde, is qualitatively the same as that for the Vaisala RS80 radiosonde (Turner et al. 2003). Thus, the MWR PWW measurements can be used as a basis for developing a correction that eliminates the daytime dry bias in the column-integrated PWV.

## 3. Daytime dry bias in column-integrated water vapor measurements at ARM SGP

Turner et al. (2003), using RS80-H sondes, noted that the daytime MWR scale factor was typically 3%–4%

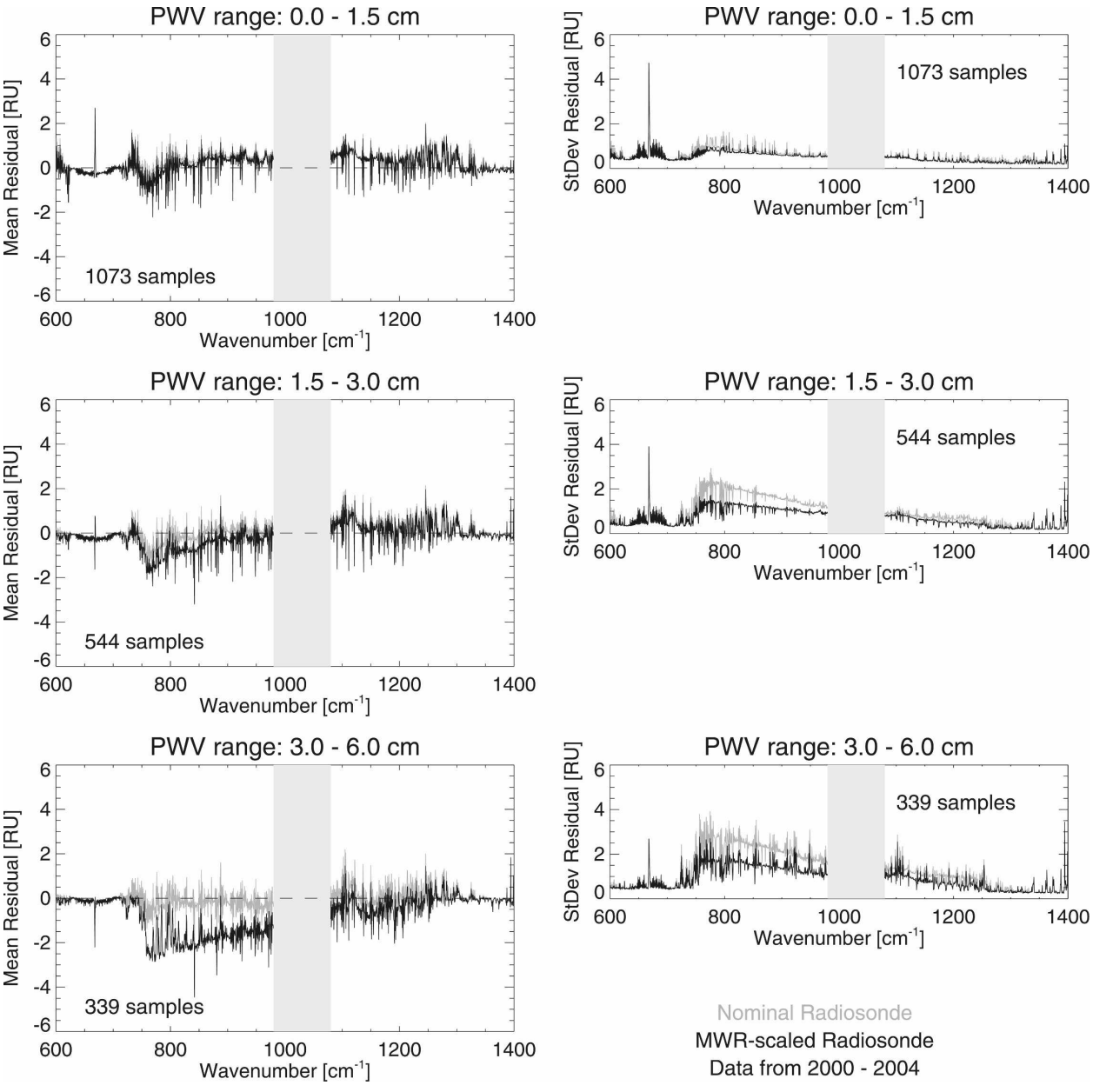


FIG. 1. (left) Mean AERI minus LBLRTM residuals and (right) std dev about the mean residual for unscaled sonde (gray) and MWR-scaled sonde (black), binned by water vapor amount. RU (mW $m^{-2}$ sr $cm^{-1}$).

higher than the nighttime factor. Measurements taken during the AWEX-G campaign at the ARM SGP site in 2003 (Miloshevich et al. 2006), for which RS90/92 sondes were used, showed that the MWR scale factor was on average 6%–8% higher during the day. The daytime dry bias has been attributed to solar heating of the sensor, which is more evident in the RS90/92 profiles because of the absence of a protective cap on these sensors: an aluminized plastic cap was used on the RS80s to shield the sensor from precipitation and solar radiation. From comparisons of Cryogenic Frostpoint Hygrometer (CFH) and Vaisala RS92 soundings taken during the Ticosonde campaign (Vömel et al. 2007) found that the daytime dry bias increases with altitude and can reach 50% near the tropopause; they constructed an empirical correction factor based on pressure, which when applied to the RS92 profiles greatly reduced the difference with respect to the CFH. However, the Vömel et al. (2007) radiative correction factor was derived for instruments ascending more rapidly

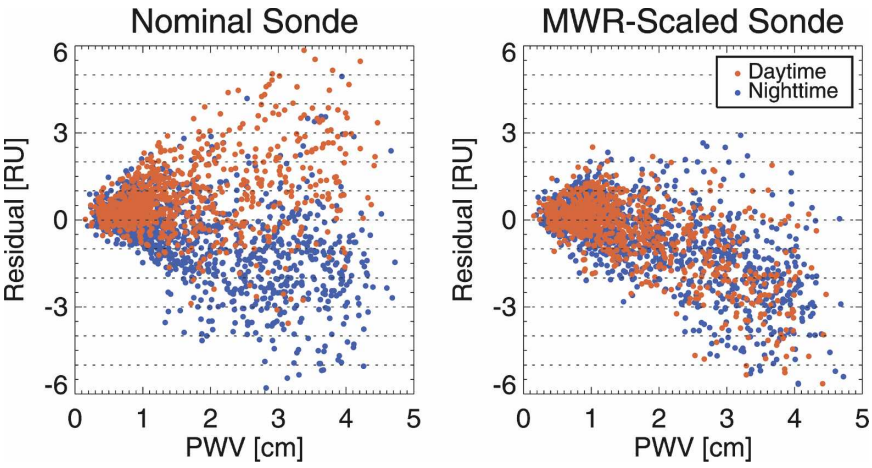


FIG. 2. AERI minus LBLRTM residuals in the 845 $cm^{-1}$ microwindow for (left) unscaled and (right) MWR-scaled sonde profiles as a function of water vapor amount. Daytime (1200–2400 UTC) residuals are in red; nighttime (0000–1200 UTC) residuals are in blue.

than usual; the faster rising leads to greater forced cooling of the sensor, thereby reducing the solar heating effect; thus, the correction factor is probably a lower estimate of the error due to solar heating. Moreover, it was derived in a tropical climate regime, for small solar zenith angles, limiting its applicability to other regions.

Our goal was to develop a simple correction scheme for the daytime dry bias in RS80-H/90/92 sondes that did not require coincident MWR measurements and was valid over a large range of solar zenith angles. We used the MWR PWV as truth, based on the results of the radiative closure experiments described in section 2, to determine the appropriate correction. The MWR Retrieval (MWRRET) dataset (Turner et al. 2007; available from the ARM IOP archive) provides, among other variables, PWV derived from radiosonde profiles, MWR brightness temperatures, and PWV and CLW retrievals from the MWR observations from 1996 through 2005. This long-term, consistent, and carefully quality-controlled dataset is an ARM value-added product (VAP), which utilizes monoRTM, a monochromatic version of LBLRTM, as a forward model, and retrieves PWV and CLW from the MWR using two different approaches: a physical retrieval and an advanced statistical retrieval. The physically retrieved PWV from MWRRET has an estimated accuracy of 0.07 cm (Turner et al. 2007). This product provides the ideal platform for examining the RS80-H/90/92 daytime bias as the solar zenith angle ranges from 20° to 90° and the retrieval algorithm is constant. We analyzed all sonde profiles from the 1998–2005 period and compared the sonde PWV with the PWV retrieved from MWR measurements averaged over a 40-min window centered around the sonde launch times. We retained only sondes launched when there was no detectable liquid cloud. We used the variability in the 31.4-GHz measurement and the MWR CLW to determine if there were liquid clouds present during the sonde ascent, following Turner et al. (2007). Figure 3 shows the monthly mean of the ratio of the MWR to sonde PWV measurements over the 1998–2005 period, plotted separately for daytime and nighttime profiles; a profile is considered to be a daytime profile if the solar zenith angle at launch time is less than 90°. Only ratios between 0.75 and 1.25 were included in the averaging. The error bars

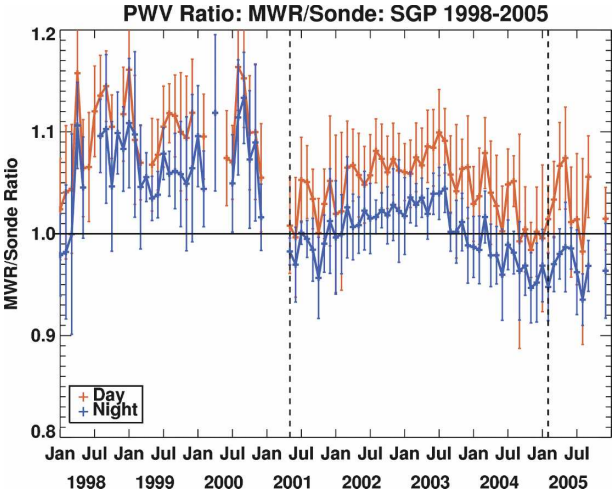


FIG. 3. Monthly averages of the ratio of the PWV retrieved from the MWR to the radiosonde PWV (MWR scale factors) collected in the absence of liquid cloud at SGP from 1998 through 2005. The dashed line in 2001 indicates transition from RS80-H to RS90 sondes; the dashed line in 2005 indicates the transition from RS90 to RS92. Error bars show std dev for each month. Daytime data (SZA less than 90°) are in red; nighttime data are in blue.

show the standard deviation of the ratio for each month. Gaps indicate months with fewer than 10 acceptable sonde profiles. The dotted lines show the transition time at the ARM SGP site from RS80-H to RS90 (May 2001) and from RS90 to RS92 (February 2005). The drop in the overall dry bias after the RS80-H–RS90 transition is very marked. This time series clearly demonstrates the existence of daytime–nighttime differences: relative to the MWR, daytime sonde profiles are consistently drier than nighttime radiosondes over the entire 2001–05 period. The monthly average RS90/92 sonde measurements were from 2% to 9% drier than the monthly average nighttime ratios over the May 2001–July 2005 period. This range brackets the 6%–8% factor reported by Miloshevich et al. (2006).

The daytime dry bias has been attributed to solar heating of the radiosonde's humidity sensor and thus is expected to have a fairly simple dependence on solar zenith angle. Other factors can also play a role, such as the ascent rate or the presence of high cirrus clouds and/or aerosols. However, we are looking for a straightforward correction that would, in general, eliminate most of the daytime dry bias. Before exploring this dependence, it is necessary to examine the "batch-to-batch" variability, which Turner et al. (2003) found to be quite high for the RS80-H sonde profiles but has not been looked at extensively for RS90/92 profiles. A batch is defined as the set of sondes calibrated in the same week (see the appendix for the algorithm that determines the batch week from the serial number). Figure 4 shows the nighttime mean of the MWR factor for each batch of RS90 and RS92 sondes deployed at SGP during the 2001–05 period, as a function of the batch ID, which is directly related to the date of manufacture (see the appendix). Within each batch, the standard deviation can be as large as 8%. The mean MWR factor for each batch appears to drift slowly with time, ranging from 0.93 to 1.04, significantly less than the 0.98–1.24 range that Turner et al. (2003) found in the RS80-H analysis. Combining the within-batch and between-batch variability could result in differences among radiosonde PWV measurements as great as 18%. We eliminated most of the drift by dividing the MWR scale factor for each sonde by the mean nighttime MWR scale factor of its batch. The adjusted MWR factors were then binned by solar zenith angle (SZA) in 5° bins, and the median and quartile values were plotted (Fig. 5). The nighttime values are shown to highlight the different character of the daytime and nighttime MWR factors.

The daytime MWR scale factor increases sharply with decreasing solar zenith angle, until SZA is ~70°, then generally rises more slowly as the SZA continues

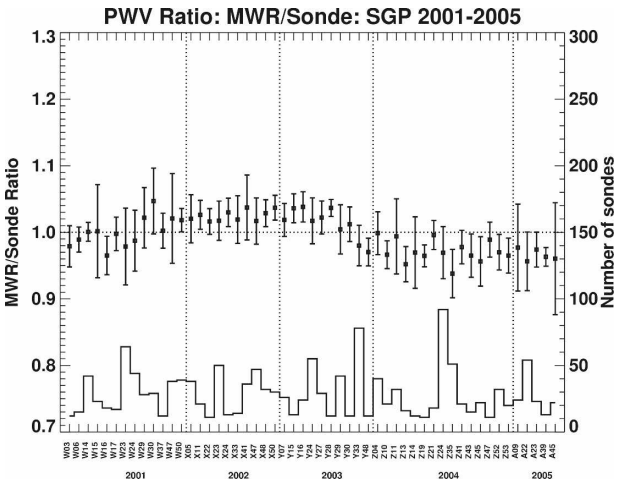


FIG. 4. Nighttime MWR scale factors for RS90/92 sondes launched in the absence of liquid cloud at SGP during the 2001–05 period. Squares indicate the mean of each batch; error bars indicate the std dev. The histogram shows the number of sondes used from each batch, and dashed lines separate years of manufacture.

to decrease. This behavior is similar to the dependence of atmospheric transmittance on air mass, as would be expected if daytime dry bias were due to solar heating. We assumed the MWR factor ($S$) would obey a function of the form given by

$$S = 1.0 + \alpha \times \exp[-\text{tau\_eff} \times \sec(\text{SZA})], \quad (1)$$

where $\alpha$ represents the effect of heating on the sensor, tau_eff is the effective optical depth over the entire

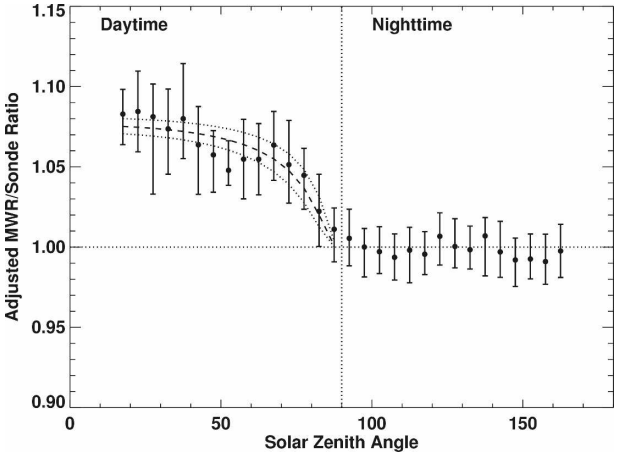


FIG. 5. MWR scale factor for the RS90/92 sondes launched in the absence of liquid cloud at SGP from 2001 through 2005, scaled by mean nighttime-batch MWR scale factor and binned by SZA. Circles indicate the median value in each bin; bars indicate the quartiles above and below the median. The dashed line is given by $1.0 + 0.093 \times \exp[-0.2\sec(\text{SZA})]$. Dotted lines bracket the range of the MWR scale factor for tau_eff, varying from 0.14 (above dashed line) to 0.26 (below dashed line).

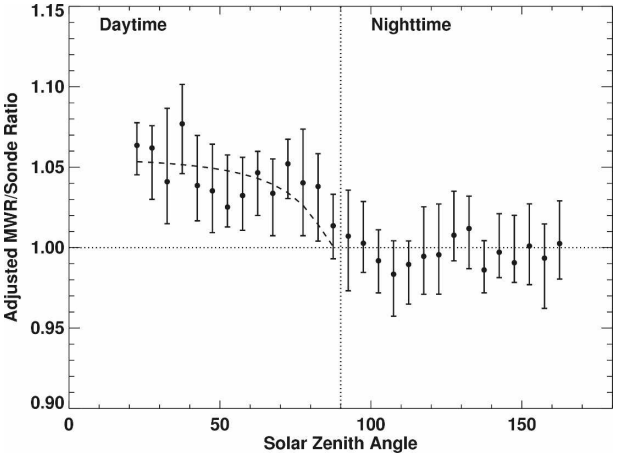


FIG. 6. MWR scale factor for the RS80-H sondes launched in the absence of liquid cloud at SGP from 1998 through 2001, scaled by mean nighttime-batch MWR scale factor and binned by SZA. Circles indicate the median value in each bin; bars indicate the quartiles above and below the median. The dashed line is given by $1.0 + 0.067 \times \exp[-0.2\sec(\mathrm{SZA})]$.

shortwave spectrum, and sec is the trigonometric function 1/cos. To determine tau_eff, we analyzed a year's worth of broadband radiative transfer runs performed by the ARM Broadband Heating Rate Profile project (BBHRP; Mlawer et al. 2002) under cloud-free conditions using profiles from the SGP site. We looked at the log of the ratio of the shortwave downward flux at the surface to the flux at TOA (the effective optical depth, tau_eff) and found that tau_eff ranged from 0.14 to 0.24, with a mean around 0.19 and a standard deviation of 0.06. We set tau_eff to 0.2 and included this value in a least squares determination of $\alpha$, using the daytime MWR factors binned by solar zenith angle, to yield $\alpha = 0.093 \pm 0.0036$. This correction is shown as a dashed line in Fig. 5, while dotted lines show the variability of the scale factor over the range of tau_eff derived from the BBHRP dataset.

Given the number of RS80-Hs still in use, it is helpful to repeat the analysis using the RS80-H radiosondes from the 1998–2001 period at the ARM SGP site. The dependence of the MWR factor on SZA for the RS80-Hs is evident, though not as pronounced (Fig. 6); using the same tau_eff, a least squares calculation yielded an alpha of $0.067 \pm 0.0065$. Because this number is proportional to the thermal absorption by the sensor, the smaller value obtained for the RS80-H radiosondes is consistent with the existence of an aluminized plastic protective cap on these sondes, which reduces the effect of solar insolation. Thus, the daytime dry bias can be removed from the R80-H and RS90/92 radiosondes through the use of one correction formula [Eq. (1)] with different values for the $\alpha$ parameter.

To test the effectiveness of this correction, all the RS80-H/90/92 daytime sonde PWV values were scaled by the function given in Eq. (1), and the MWR factors were recalculated. A scatterplot of the MWR and RS90/92 sonde PWV with and without the solar zenith correction (Fig. 7) shows that slope becomes closer to 1 when the correction is applied, indicating that the day-

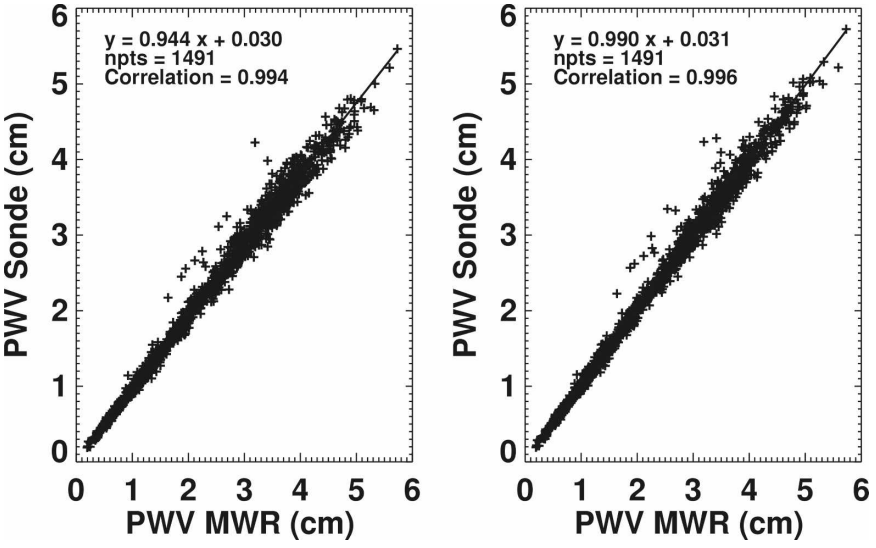


FIG. 7. For daytime cases, scatterplots of (left) uncorrected sonde PWV and (right) corrected sonde PWV vs MWR PWV. All sonde measurements are from RS90/92 sondes. The uncorrected scatterplot has a slope of 0.94 and an RMS of 0.054, while the corrected scatterplot has a slope of 0.99 and an RMS of 0.048.

time dry bias has been significantly reduced. The mean MWR factor for the unscaled sondes is 1.044, which decreases to 0.99 for the scaled sondes. Further evidence of the effectiveness of the solar zenith correction technique is evident in Fig. 8, where the daytime RS80-H/90/92 sonde PWVs have now been corrected by the SZA function. The monthly means of the corrected daytime MWR factors now track the nighttime means much more closely; note that this correction does not remove any dry bias due to factors other than solar heating: the RS80-H dry bias is still very evident. There are still significant differences in early 2005, right after the switch to the RS92 sensors; these differences appear to decrease later in 2005. The marked drop in the daytime dry bias when the radiosonde humidity profiles are corrected by the solar zenith angle function confirms that this simple technique is an effective tool for removing most of the daytime dry bias in the sonde column-integrated PWV when there is no MWR available.

The analysis just described focused on a long-term dataset at a single location. While this dataset encompassed a wide range of solar zenith angles (16°–90°) and PWV (0.2–5.7 cm) values, there were few profiles with high PWV (greater than 5 cm) or taken at SZA less than 20°. With the objective of testing the general applicability of the SZA correction described above, we repeated the entire analysis for another MWRRET dataset, collected at the ARM Tropical Western Pacific (TWP) sites at Nauru and Darwin, Australia, during the 2002–06 period. Here more than 50% of the profiles have PWV greater than 5 cm, and 80 profiles were collected at SZA less than 20°. All radiosondes were RS90/92. The daytime dry bias in the sondes is again very evident (Fig. 9); the daytime MWR factors present a similar dependence on solar zenith angle (Fig. 10); finally the same correction function applied to the SGP dataset eliminates the daytime bias (Fig. 11). This confirms the applicability of the correction to locations with insolation and humidity characteristics that are very different from the southern Great Plains.

The preceding application examples have qualitatively validated the proposed correction. A more quantitative estimate of the upper limit of the error in the PWV may be obtained by calculating the uncertainty in the MWR factor for a humid (5-cm PWV) profile at low SZA (5°). The error in the MWR is 0.07 cm (Turner et al. 2007); from the standard deviations obtained from the determination of tau_eff and alpha, the expected error in the MWR factor for this profile is 0.007; assuming that the errors in the MWR and the correction algorithm [Eq. (1)] are independent, one obtains an error of 0.08 cm in PWV for this case with very significant solar heating.

As stated earlier, cases with liquid water clouds were removed from the analysis using the screening technique in Turner et al. (2007). Because only MWR data are used in this screening technique, in which the brightness temperature observations at 23.8 and 31.4 GHz are insensitive to ice, scenes with ice clouds are included in this analysis. Therefore, the empirical cor-

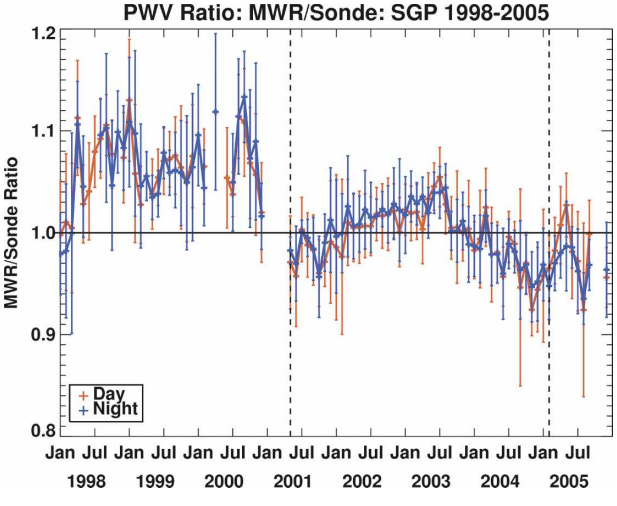


FIG. 8. MWR scale factor: monthly averages from data collected in the absence of liquid cloud at SGP from 1998 through 2005. The dashed line in 2001 indicates transition from RS80-H to RS90; the dashed line in 2005 indicates transition from RS90 to RS92. Daytime sondes scaled by 1.0 + alpha × exp[−0.2sec(SZA)], where alpha is 0.067 before May 2001 and 0.093 thereafter.

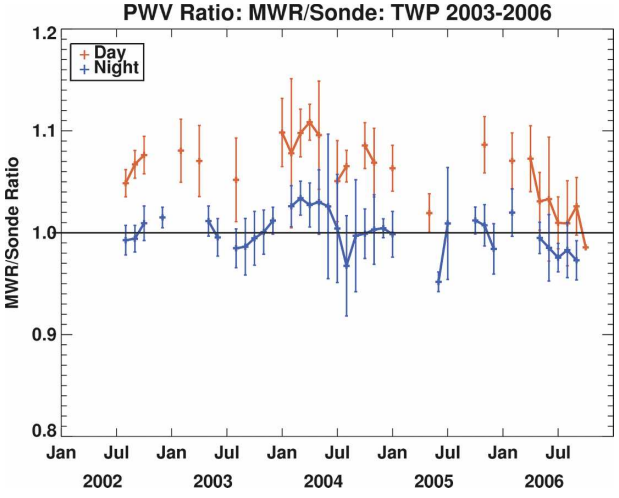


FIG. 9. MWR scale factor: monthly averages from data collected in the absence of liquid cloud at the Republic of Nauru from 2002 through 2005 and at Darwin, Australia, in 2006. Error bars show the std dev for each month.

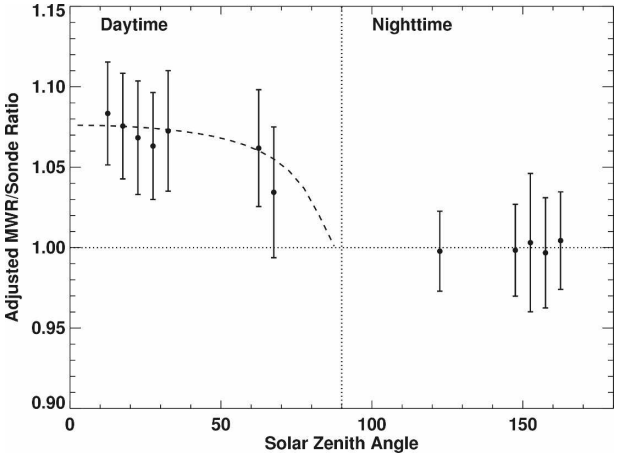


FIG. 10. MWR scale factor for the RS90/92 sondes launched in the absence of liquid cloud at Nauru and Darwin from 2002 through 2006, scaled by mean nighttime-batch MWR factor and binned by SZA. Circles indicate median value in each bin; bars indicate the quartiles above and below the median. The dashed line is given by $1.0 + 0.093 \times \exp[-0.2\sec(\mathrm{SZA})]$.

rection is applicable to both clear sky cases and cases in which there are overhead cirrus clouds of various optical depths.

We have so far confined our analysis to scenes with no liquid cloud, as the accuracy of the PWV retrieved from the MWR is greater when liquid clouds are nonexistent or very thin. Liquid clouds are of course extremely common—thus the possible applicability of this daytime dry bias correction methodology. Because solar radiation that may warm the humidity sensor would be significantly attenuated by liquid clouds, one would expect that the effective optical depth in Eq. (1) should increase with increasing CLW, thus leading to a reduced dry bias. To test this hypothesis, we grouped all the RS90/92 SGP observations with liquid cloud (i.e., with an MWR 31.4-GHz standard deviation above our cloudy threshold) into four CLW bins (Fig. 12); the sonde PWV daytime dry bias is evident in every CLW bin and does not appear to be very dependent on CLW. While this result is surprising and warrants further investigation, it also suggests that our proposed dry bias correction can be applied as a first-order correction in the presence of liquid clouds.

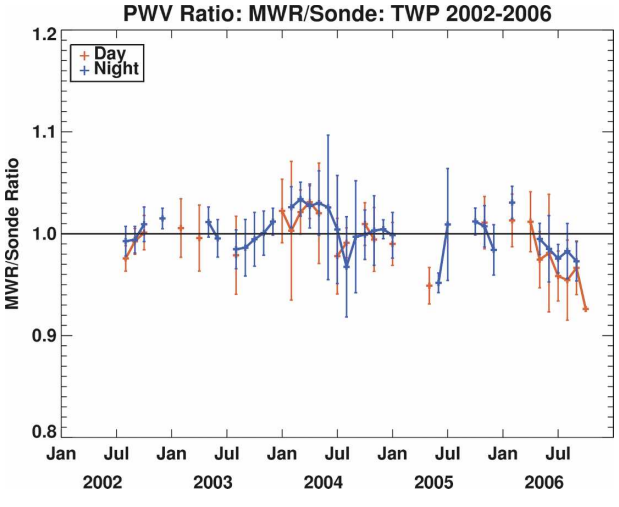


FIG. 11. MWR scale factor: monthly averages from data collected in the absence of liquid cloud at Nauru from 2002 through 2005 and at Darwin in 2006. Error bars show the std dev for each month. Daytime sondes scaled by $1.0 + 0.093 \times \exp[-0.2\sec(\mathrm{SZA})]$.

As an illustration of the importance of correcting the dry bias in the radiosonde humidity profiles, over 4.5 yr of RS90 and RS92 temperature and water vapor profiles from 1730 UTC (near local solar noon) observed over the ARM SGP site were used to calculate CAPE, both before and after MWR scaling was applied. The results are shown in Fig. 13. The MWR-scaled sonde profiles, and by extension the empirical SZA-corrected profiles, yield substantially larger CAPE values. The mean difference between the CAPE from the unscaled and scaled sonde profiles is 92.9 J $kg^{-1}$, with an RMS difference of 172.4 J $kg^{-1}$. These results are qualitatively similar to those Guichard et al. (2000) obtained in a tropical environment during TOGA COARE and demonstrate that the use of uncorrected Vaisala RS90 and RS92 radiosonde humidity profiles leads to severe underestimation of convective instability.

## 4. Summary and conclusions

Vaisala radiosondes are used for many different applications, in both research and operational settings, in the United States and abroad. Existing biases in the humidity profiles collected by these sondes will impact radiative closure experiments and the prediction and modeling of convective events, as well as long-term climate records and global change modeling efforts. Our extensive comparison of PWW measurements from the MWR and the RS90/92 sondes reiterates the value of scaling the sondes by the MWR; this scaling eliminates the batch-to-batch variability, leading to substantially less scatter in infrared radiative transfer closure studies.

Scaling the radiosonde humidity profile to agree with the MWR-retrieved PWV value also eliminates the daytime dry bias, observed by previous researchers during short campaigns such as AWEX-G and Ticosonde. However, MWR instruments are not usually available in operational settings or even during many measurement campaigns. Analysis of the daytime differences

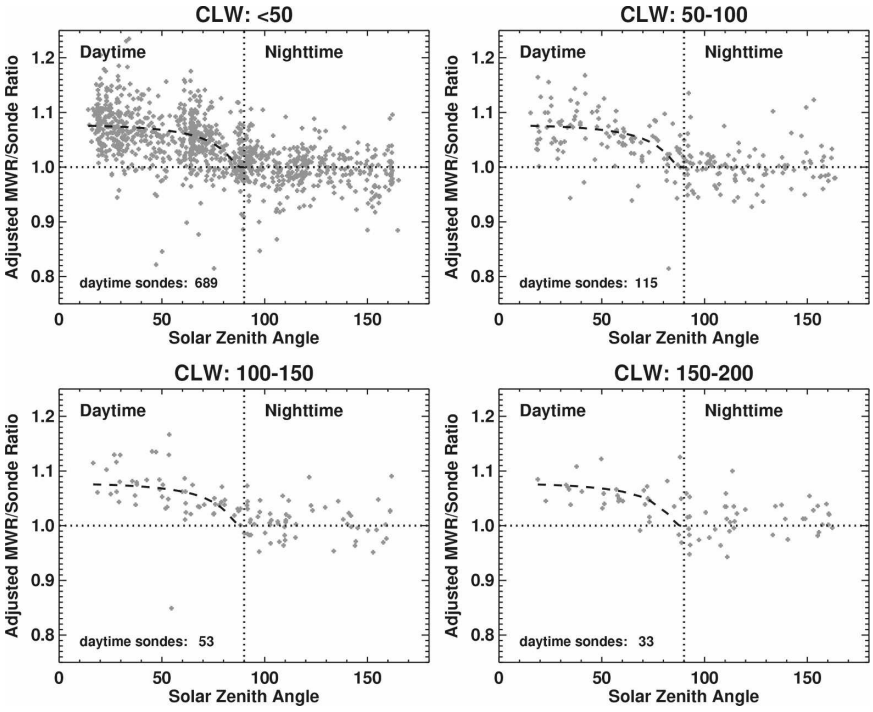


FIG. 12. MWR scale factor for the RS90/92 sondes launched from SGP from 2001 through 2005 in the presence of liquid clouds [CLW (g $m^{-2}$)]; MWR factor scaled by mean nighttime-batch MWR scale factor and binned by SZA. The dashed line is given by $1.0 + 0.093 \times \exp[-0.2\sec(\mathrm{SZA})]$.

between the MWR and the RS80-H/90/92 sondes led to a semiempirical correction based on the solar zenith angle that was shown to effectively eliminate the daytime dry bias in PWV. This correction is consistent with the assumption of solar heating of the humidity sensor, can be applied without reference to the MWR, and is valid for all solar zenith angles. The same form of the correction, with different values for the alpha parameter, appears to work equally well for RS80-H and RS90/92 sonde profiles, though the validity for the RS92s should be tested more extensively. The correction, which was derived using data at a midlatitude site with moderate amounts of water vapor and solar zenith angles, was tested successfully on data collected at tropical sites with larger amounts of water vapor and smaller solar zenith angles. Incorporating this simple correction into the processing algorithms of Vaisala RS80-H/90/92 sonde profile data will greatly increase the quality of the profiles and of the products derived from them, whether they are short-term severe weather forecasts or long-term climate change estimates.

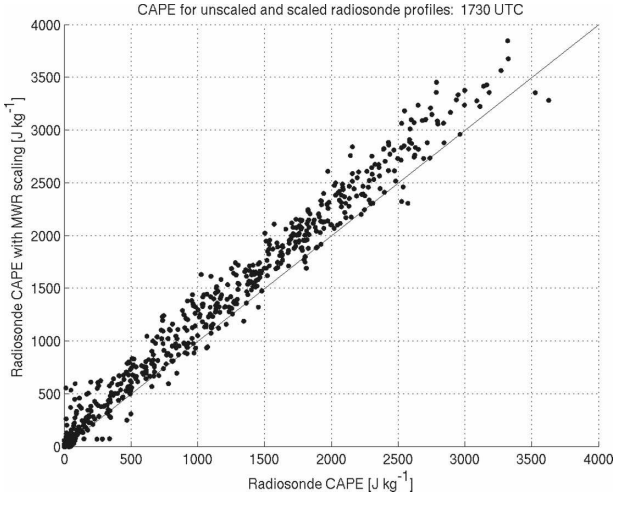


FIG. 13. CAPE from 4.5 yr of RS90 and RS92 temperature and water vapor profiles from 1730 UTC (near local solar noon) observed over the ARM SGP site both before and after MWR scaling was applied; fitting a straight line through data leads to a slope of 1.108 and an intercept of 28.016.

*Acknowledgments.* We thank J. Liljegren, who has been instrumental in creating the MWR data streams at ARM, and B. Lesht, for his management of the ARM SGP sonde launches. This research was funded by the Atmospheric Radiation Measurement (ARM) Program sponsored by the U.S. Department of Energy, Office of Science, Office of Biological and Environmental Research, Environmental Sciences Division.

## APPENDIX

### Determining Batch Production Week from Radiosonde Serial Number

Vaisala RS-9092 radiosondes (used operationally by ARM at SGP since 1 May 2001) have serial numbers coded as YWWDSSSS, where

Y = alphabetic code for the year (T = 1998, U = 1999, etc.);
WW = week number (1–52);
D = day of the week (1–7; Monday = 1); and
SSSS = sequence number.

## REFERENCES


Ackerman, T. P., and G. M. Stokes, 2003: The atmospheric radiation measurement program. *Phys. Today,* **56,** 38–44.

Clough, S. A., M. W. Shephard, E. J. Mlawer, J. S. Delamere, M. J. Iacono, K. Cady-Pereira, S. Boukabara, and P. D. Brown, 2005: Atmospheric radiative transfer modeling: A summary of the AER codes (short communication). *J. Quant. Spectrosc. Radiat. Transfer,* **91,** 233–244.

Guichard, F., D. Parsons, and E. Miller, 2000: Thermodynamic and radiative impact of the correction of sounding humidity bias in the Tropics. *J. Climate,* **13,** 3615–3624.

Knuteson, R. O., and Coauthors, 2004a: Atmospheric Emitted Radiance Interferometer. Part I: Instrument design. *J. Atmos. Oceanic Technol.,* **21,** 1763–1776.

——, and Coauthors, 2004b: Atmospheric Emitted Radiance Interferometer. Part II: Instrument performance. *J. Atmos. Oceanic Technol.,* **21,** 1777–1789.

Liljegren, J. C., 2000: Automatic self-calibration of ARM microwave radiometers. *Microwave Radiometry and Remote Sensing of the Environment,* P. Pampaloni, Ed., VSP Press, 9 pp. [Available online at http://www.arm.gov/instruments/publications/mwr_calibration.pdf.]

Miloshevich, L. M., H. Vömel, D. N. Whiteman, B. M. Lesht, F. J. Schmidlin, and F. Russo, 2006: Absolute accuracy of water vapor measurements from six operational radiosonde types launched during AWEX-G and implications for AIRS validation. *J. Geophys. Res.,* **111** D09S10, doi:10.1029/2005JD006083.

Mlawer, E. J., and Coauthors, 2002: The broadband heating rate profile (BBHRP) VAP. *Proc. 12th Atmospheric Radiation Measurement (ARM) Science Team Meeting,* St. Petersburg, FL, U.S. Department of Energy. [Available online at http://www.arm.gov/publications/proceedings/conf12/index.stm.]

Raval, A., and V. Ramanathan, 1989: Observational determination of the greenhouse effect. *Nature,* **342,** 758–761.

Revercomb, H. E., and Coauthors, 2003: The ARM program's water vapor intensive observation periods: Overview, initial accomplishments, and future challenges. *Bull. Amer. Meteor. Soc.,* **84,** 217–236.

Solomon, S., D. Qin, M. Manning, Z. Chen, M. Marquis, K. B. Averyt, M. Tignor, and, H. L. Miller, 2007: *Climate Change 2007: The Physical Basis of Climate Change.* Cambridge University Press, 1009 pp.

Turner, D. D., B. M. Lesht, S. A. Clough, J. C. Liljegren, H. E. Revercomb, and D. C. Tobin, 2003: Dry bias and variability RS80-H Radiosondes: The ARM experience. *J. Atmos. Oceanic Technol.,* **20,** 117–132.

——, and Coauthors, 2004: The QME AERI LBLRTM: A closure experiment for downwelling high spectral resolution infrared radiance. *J. Atmos. Sci.,* **61,** 2657–2675.

——, S. A. Clough, J. C. Liljegren, E. E. Clothiaux, K. E. Cady-Pereira, and K. L. Gaustad, 2007: Retrieving liquid water path and precipitable water vapor from the Atmospheric Radiation Measurement (ARM) microwave radiometers. *IEEE Trans. Geosci. Remote Sens.,* **45,** 3680–3690.

Vömel, H., and Coauthors, 2007: Radiation dry bias of the Vaisala RS92 humidity sensor. *J. Atmos. Oceanic Technol.,* **24,** 953–963.

Wang, J., H. Cole, D. J. Carlson, E. R. Miller, K. Beierle, A. Paukkunnen, and T. K. Laine, 2002: Corrections of humidity measurement errors from the Vaisala RS80 radiosonde—Applications to TOGA COARE data. *J. Atmos. Oceanic Technol.,* **19,** 981–1002.

Zipser, E. J., and R. H. Johnson, 1998: Systematic errors in radiosonde humidities: A global problem? Preprints, *10th Symp. on Meteorological Observations and Instrumentation,* Phoenix, AZ, Amer. Meteor. Soc., 72–73.